

Yang Wang, Benjamin Passey, Rupsa Roy, Tao Deng, Shijun Jiang, Chance Hannold, Xiaoming Wang, Eric Lochner, and Aradhna Tripati, 2020, Clumped isotope thermometry of modern and fossil snail shells from the Himalayan-Tibetan Plateau: Implications for paleoclimate and paleoelevation reconstructions: GSA Bulletin, <https://doi.org/10.1130/B35784.1>.

## Supplemental Material

**Supplementary Table S1.** Summary of temperatures calculated using carbonate clumped isotope thermometry on modern Tibetan freshwater snail shells.

**Supplementary Table S2.** XRD analysis results of fossil shells from the Tibetan Plateau.

**Supplementary Table S3.** Summary of temperatures calculated using carbonate clumped isotope thermometry on fossil shells from Tibetan Plateau.

**Supplementary Table S4.** Comparison of temperatures calculated using different equation.

**Supplementary Figure S1.** Comparison of analysis results for fossils (A–C) and modern shells (D) analyzed in different labs. The double arrows in (A) and (B) indicate the variation ranges of  $\delta^{13}\text{C}$  and  $\delta^{18}\text{O}$  values, respectively, of modern shells. Temperatures shown in (C) and (D) were calculated using the Henkes et al. (2013) calibration. The error bar indicates 1 standard deviation from the mean of replicated analyses of a sample. Some of the fossil samples analyzed at Caltech and John Hopkins University (JHU) were re-analyzed at University of Michigan (UM), yielding the same  $\delta^{13}\text{C}$  and  $\delta^{18}\text{O}$  values and similar  $\Delta_{47}$ -derived temperature values for the same samples (A–C). Analysis of additional modern samples from two of the study lakes at UCLA also produced similar results to those from the JHU lab for the same lakes except two samples (D). The results from these two samples analyzed at UCLA were not used because their replicates yielded not only very large temperature ranges (much larger than the reported analytical uncertainty) but also unreasonably high temperatures (see text for explanation).

**Supplementary Figure S2.** Effect of mixing diagenetic calcite with pristine aragonite on the  $\Delta_{47}$ -derived temperature of aragonite shell predicted using a simple two component mixing model. The model assumes that calcite was formed at near freezing temperatures (1°C) characterizing the present-day high elevation environment in the study area and the temperature of unaltered aragonite was the average temperature determined from the  $\Delta_{47}$  values of our pristine fossil shells from Zanda Basin in southwest Tibet.

**Supplementary Figure S3.** Modeled  $\Delta_{47}$  evolution at low temperatures using Eq. (3) in Staudigel and Swart (2016) and rates calculated by the Arrhenius Equation. The following Arrhenius parameters estimated by Staudigel and Swart (2016) were used to calculate the rate constants at different temperatures:  $E_a = 1.1 \times 10^5 \text{ J/mol}$ , and  $\ln(k_0) = 21.7$ . The initial  $\Delta_{47}$  value used in the model was assumed to be 0.625 and the equilibrium or “annealing” values at different temperatures were calculated using the revised carbonate equation given in Zaarur et al. (2013):  $\Delta_{47} = (0.0526 \pm 0.0025) \times 1000000/T^2 + (0.0520 \pm 0.0284)$ .

Supplementary Table 1. Summary of temperatures calculated using carbonate clumped isotope thermometry on modern Tibetan freshwater snail shells

Sample ID	Latitude, Longitude	Elev. (m)	$\delta^{13}\text{C}$ (‰ vs. VPDB)	$\delta^{18}\text{O}$ (‰ vs. VPDB)	$\Delta_{47}$ (‰) (Caltech)*	$\Delta_{47}$ (‰) (ARF)**	$^a\text{T}$ (°C) (Henkes calibration)	Sample average T (°C) (Henkes calibration )	$\pm 1\sigma$ (°C) #	Calculated $\delta^{18}\text{O}$ of water (‰ vs. VSMOW)	$^b\text{T}$ (°C) (Eagle calibration)	Sample average T (°C) (Eagle calibration)	$\pm 1\sigma$ (°C) #	Calculated $\delta^{18}\text{O}$ of water (‰ vs. VSMOW)	No. of replicate analyses
<b>Samples analyzed at JHU:</b>															
	N31°41'36.200 " E88°42'10.811	4580	-0.1	-2.3		0.729	12.8	13		-3.3	18.0	18		-2.2	1
Cuo-er	"														
Nam1s-1	N30° 43' 9.19", E90° 55' 13.39"	4700	-11.0	-14.4		0.744	7.3	7		-16.6	13.3	13		-15.3	1
Nam1s-2	N30° 43' 9.19", E90° 55' 13.39"	4700	-11.0	-13.5		0.728	12.9	13		-14.5	18.1	18		-13.4	1
Nam1s-3	N30° 43' 9.19", E90° 55' 13.39"	4700	-10.5	-13.8		0.755	3.8	9	7	-15.7	10.3	15	6	-14.4	2
Nam1s-3rp1						0.725	14.0				19.0				
Nam1s-4	N30° 43' 9.19", E90° 55' 13.39"	4700	-10.0	-13.3		0.717	17.0	16	1	-13.6	21.5	21	1	-12.6	2
Nam1s-4rp1						0.721	15.4				20.1				
QGC-1	N31°50.33913', E88°20.26378"	4560	-1.0	-4.3		0.718	16.7	17		-4.5	21.3	21		-3.5	1
QGC-2	N31°50.33913', E88°20.26378'	4560	-0.3	-3.9		0.734	10.9	11		-5.3	16.3	16		-4.1	1
SLC-1	N31°47.63722', E88°27.01484'	4555	-4.0	-3.4		0.759	2.6	7	5	-5.6	9.2	13	4	-4.3	3
SLC-1rp1						0.728	12.9				18.0				
SLC-1rp2						0.746	6.7				12.8				
SLC-2	N31°47.63722', E88°27.01484'	4555	0.5	-7.0		0.734	10.7	9	2	-8.7	16.2	15	2	-7.5	2

SLC-2rp1		0.5	-6.9	0.742	8.0				13.9				
Yam2s-1	N29.099777°, E90.375814°	4420	-7.7	-15.5	0.731	11.8	14	4	-16.1	17.1	19	3	-15.1
Yam2s-1rp1			-7.7	-15.5	0.717	17.0				21.5			
Yam2s-2	N29.099777°, E90.375814°	4420	-9.6	-15.8	0.743	7.6	10	4	-17.3	13.6	16	3	-16.1
Yam2s-2rp1			-9.6	-15.8	0.727	13.2				18.3			
Yam2s-3	N29.099777°, E90.375814°	4420	-9.6	-15.8	0.733	11.3	11		-17.1	16.7	17		-15.9
Yam2s-4	N29.099777°, E90.375814°	4420	-8.1	-15.4	0.729	12.6	11	2	-16.7	17.8	17	1	-15.6
Yam2s-4rp1			-8.1	-15.4	0.736	10.2				15.8			
YXC-1	N34°17'12.8", E92°40'52.9"	4520	-1.5	-5.2	0.741	8.4	8		-7.2	14.2	14		-5.9
YXC-3	N34°17'12.8", E92°40'52.9"	4520	-0.9	-4.3	0.729	12.8	13		-5.3	18.0	18		-4.2
YXC-4	N34°17'12.8", E92°40'52.9"	4520	-0.6	-6.0	0.744	7.5	8		-8.1	13.5	13		-6.8
YXC-5-1	N34°17'12.8", E92°40'52.9"	4520	0.8	-5.6	0.750	5.3	1	4	-9.3	11.5	8	4	-7.7
YXC-5-1rp1			0.8	-5.6	0.767	0.0				7.0			
YXC-5-1rp2			0.6	-5.5	0.777	-3.2				4.2			
YXC-5-2	N34°17'12.8", E92°40'52.9"	4520	-0.8	-6.8	0.737	9.8	8	2	-8.8	15.4	14	2	-7.5
YXC-5-2rp1			-0.8	-6.7	0.747	6.5				12.6			
YXC-5-3	N34°17'12.8", E92°40'52.9"	4520	-1.4	-6.2	0.733	11.2	7	6	-8.5	16.7	13	5	-7.1
YXC-5-3rp1			-1.4	-6.3	0.757	3.2				9.8			
YXC-5-4	N34°17'12.8", E92°40'52.9"	4520	-0.9	-5.8	0.739	9.1	5	5	-8.5	14.8	12	4	-7.1
YXC-5-4rp1			-0.9	-5.9	0.761	1.8				8.6			

TB07S-1	N30°43'54.7", E81°36'07.2"	4590	-4.3	-3.9	0.676		8.1	8	1	-6.1	13	13	1	-4.9	2
TB07S-1(rpt.)			-4.3	-3.9	0.679		7.0				12				
TB07S-1a	N30°43'54.7", E81°36'07.2"	4590	-4.6	-4.1	0.666		11.5	11		-5.4	16	16		-4.3	1

**Samples analyzed at UCLA:**

YAM-16-2-2	N29°05'52.6" E90°22'44.4"	4430	-4.8	-7.8		0.742	8.1	8		-9.8	14.0	14		-8.5	1
YAM-16-2-3, R1	N29°05'52.6" E90°22'44.4"	4430	-7.79	-14.48		0.718	16.6	13	6	-15.5	21.2	18	5	-14.4	2
YAM-16-2-3, R2			-7.77	-14.42		0.74	8.8				14.6				
YAM-16-3-1, R1	N29°11'13.1" E90°35'26.9"	4435	-0.32	-4.3		0.717	17.0	10	5	-5.8	21.5	16	4	-4.6	4
YAM-16-3-1, R2			-0.25	-4.16		0.745	7.1				13.1				
YAM-16-3-1, R3			-0.25	-4.15		0.749	5.7				12.0				
YAM-16-3-1, R4			-0.24	-4.16		0.733	11.2				16.6				
YAM-16-3-2, R1	N29°11'13.1" E90°35'26.9"	4435	-0.18	-4.01		0.743	7.8	6	8	-6.4	13.7	12	7	-5.1	4
YAM-16-3-2, R2			-0.18	-3.98		0.729	12.6				17.8				
YAM-16-3-2, R3			-0.13	-3.87		0.784	-5.2				2.5				
YAM-16-3-2, R4			-0.38	-4.39		0.734	10.9				16.3				
YAM-16-3-3, R2	N29°11'13.1" E90°35'26.9"	4435	-0.58	-4.87		0.72	15.9	16	5	-5.2	20.6	21	4	-4	3
YAM-16-3-3, R3			-0.6	-4.93		0.707	20.8				24.7				
YAM-16-3-3, R4			-0.85	-5.35		0.733	11.2				16.6				
YAM-16-3-3, R1			-0.56	-4.83		0.691	27.2				30.1				4
T16-05G-1, R1	N30°43'58.3" E81°36'05.6"	4600	-3.590	-3.720		0.739	9.1	13	4	-4.7	14.8	18	3	-3.6	

T16-05G-1, R2		-3.550	-3.630	0.729	12.6				17.8				
T16-05G-1, R3		-3.540	-3.710	0.717	17.0				21.5				
T16-05G-2, R1	N30°43'58.3" E81°36'05.6"	4600	-3.19	-3.52	0.708	20.4	9	9	-5.4	24.4	14	7	-4.2
T16-05G-2, R2			-3.15	-3.48	0.752	4.8			11.1				
T16-05G-2, R3			-3.35	-3.96	0.765	0.6			7.5				
T16-05G-2, R4			-3.19	-3.59	0.741	8.4			14.3				
T16-05G-3, RI	N30°43'58.3" E81°36'05.6"	4600	-4.53	-2.49	0.704	22.0	17	12	-2.6	25.7	21	10	-1.8
T16-05G-3, R4			-4.63	-2.86	0.771	-1.3			5.9				
T16-05G-3, R5			-4.42	-2.45	0.707	20.8			24.7				
T16-05G-3, R2			-4.45	-2.38	0.694	26.0			29.0				
T16-05G-4, RI	N30°43'58.3" E81°36'05.6"	4600	-3.87	-3.31	0.698	24.4	22	9	-2.3	27.7	26	7	-1.6
T16-05G-4, R2			-3.83	-3.29	0.728	13.0			18.1				
T16-05G-4, R3			-3.79	-3.32	0.685	29.8			32.1				

**Holocene and modern shells analyzed by Huntington et al. (2015):**

nrc10-107-1	4830	-2.5	-9.1	0.679		7	3	-11.4		12	3	-10.2	
nrc10-114-4	4830	-4.4	-12.1	0.660		14	3	-12.9		18	3	-11.9	
nrc10-108-2	4810	-2.6	-7.5	0.660		14	2	-8.3		18	2	-7.3	
.2507-06-5	4880	-4.2	-3.8	0.689		4	2	-6.9		9	2	-5.5	
DT 10-9-3	4550	-9.1	-7.8	0.626		27	4	-5.8		30	4	-5.3	
Zhongba 10-7-2	4570	-5.2	-15.3	0.664		12	3	-16.4		17	3	-15.4	

Zhongba 10-6b	4570	-7.6	-10.8	0.624		28	3	-8.7		31	3	-8.1
Zhongba 10-10a	4570	-5.8	-16.1	0.653		16	3	-16.3		21	3	-15.5
Tsangpo 27	4580	-4.0	-17.7	0.658		15	3	-18.3		19	3	-17.4

\*Data reported relative to the previous 'Ghosh' scale (Ghosh et al., 2006). Uncertainty is  $\pm 0.025\%$  (95% confidence interval).

\*\*Data reported relative to the absolute reference frame (ARF) (Dennis et al., 2011). Uncertainty is  $\pm 0.017\%$  (95% confidence interval).

<sup>#</sup> One standard deviation from the mean of replicate analyses of the same sample.

<sup>a</sup> Temperatures calculated from  $\Delta_{47}$  values using the mollusk-specific calibration of Henkes et al. (2013):  $\Delta_{47} = 32700/T^2 + 0.3286$  for new data (on ARF scale), and  $\Delta_{47} = 31800/T^2 + 0.2737$  for  $\Delta_{47}$  data on "Ghosh" scale. Uncertainty in reported temperatures is  $\pm 6^\circ\text{C}$  (95% confidence interval).

<sup>b</sup> Temperatures calculated from  $\Delta_{47}$  using the 'Aragonitic bivalve mollusks' calibration of Eagle et al (2013):  $\Delta_{47} = 40700/T^2 + 0.2483$  for new data in ARF;  $\Delta_{47} = 38300/T^2 + 0.2094$  for data on the "Ghosh" scale.

Note: The last two samples (highlighted in italic) analyzed in the UCLA lab were not included in the calculation of the average  $\Delta_{47}$  - temperature values for modern samples because replicate analyses of these two samples yielded not only a very large temperature range of  $28^\circ\text{C}$  (from  $-1.3$  to  $26^\circ\text{C}$ ) for T16-05G-3 and of  $17^\circ\text{C}$  (from  $13$  to  $30^\circ\text{C}$ ) for T16-05G-4, both of which are much larger than the reported analytical uncertainty ( $\pm 6^\circ\text{C}$ ), but also unreasonably high temperatures that exceed the observed maximum lake water temperature.

Supplementary Table 2. XRD analysis results of fossil shells from the Tibetan Plateau

Sample ID	Type	Locality	Estimated Ages	%Aragonite	%Calcite*
TB07S-20a	broken whole shell	Zanda	4.2 Ma	99.65	0.35
TB07S-20b	whole shell	Zanda	4.2 Ma	99.88	0.12
TB07S-20c	whole shell	Zanda	4.2 Ma	99.84	0.16
TB07S-24a	broken whole shell	Zanda	5.1 Ma	99.79	0.21
TB07S-24b	whole shell	Zanda	5.1 Ma	99.80	0.20
TB07S-24c	whole shell	Zanda	5.1 Ma	99.46	0.54
ZD0710/TB07S-9	broken whole shell	Zanda	3.7 Ma	99.11	0.89
TB07S-9a	broken whole shell	Zanda	3.7 Ma	99.48	0.52
TB07S-9b	broken whole shell	Zanda	3.7 Ma	99.67	0.33
TB07S-13a	broken whole shell	Zanda	3.3 Ma	99.60	0.40
TB07S-13b	whole shell	Zanda	3.3 Ma	99.46	0.54
TB07S-6	whole shell	Zanda	4 Ma	99.44	0.56
TB07S-6a	whole shell	Zanda	4 Ma	99.25	0.75
TB07S-6b	whole shell	Zanda	4 Ma	99.68	0.32
TB07S-6c	whole shell	Zanda	4 Ma	99.68	0.32
TB07S-6d	whole shell	Zanda	4 Ma	99.60	0.40
TB07S-25a	broken whole shell	Zanda	5.3 Ma	99.64	0.36
TB07S-25b	broken whole shell	Zanda	5.3 Ma	99.34	0.66
TB07S-19a	broken whole shell	Zanda	4.4 Ma	99.60	0.40
TB07S-19b	whole shell	Zanda	4.4 Ma	99.85	0.15
TB07S-19c	broken whole shell	Zanda	4.4 Ma	99.65	0.35
TB07S-19d	broken whole shell	Zanda	4.4 Ma	99.81	0.19
TB07S-21a	whole shell	Zanda	4.3 Ma	99.74	0.26
TB07S-21b	broken whole shell	Zanda	4.3 Ma	98.80	1.20
KL-shell-1	mixture of several shell fragments	Kunlun Pass	3.6-4.2 Ma	99.51	0.49
KLPS-15-shells	mixture of several shell fragments	Kunlun Pass	3.6-4.2 Ma	N/A	
CD11031	whole shell	Quan-ji	Late Pleistocene	99.81	0.19
CD11031r	whole shell	Quan-ji	Late Pleistocene	99.81	0.19
DT1304a	small shell (~0.8cm)	Nie-la-mu	Late Miocene	54.85	45.15
DT1304b	shell fragment	Nie-la-mu	Late Miocene	99.21	0.79
Lun-1b	shell fragment	Lunpola Basin	Early Miocene	100.00	0.00
Lun-1c	shell fragment	Lunpola Basin	Early Miocene	99.80	0.20
Lun-1d	shell fragment	Lunpola Basin	Early Miocene	99.32	0.68
Lun-1e	shell fragment	Lunpola Basin	Early Miocene	99.47	0.53

\* The detection threshold is 0.3-0.4%. Samples with %calcite <0.4% are considered pristine.

Supplementary Table 3. Summary of temperatures calculated using carbonate clumped isotope thermometry on fossil shells from Tibetan Plateau

Sample ID	Locality	Estimated Age (Ma)	%Calcite	$\delta^{13}\text{C}$ (‰)	$\delta^{18}\text{O}$ (‰)	$\Delta_{47}$ (‰) (Caltech)*	$\Delta_{47}$ (‰) (ARF)**	<sup>a</sup> T (°C) (Henkes Cal)	Calculated $\delta^{18}\text{O}$ of water (‰)	<sup>b</sup> T (°C) (Eagle Cal)	Calculated $\delta^{18}\text{O}$ of water (‰)	Note
KL-Shell-1	Kunlun Pass	3.6-4.2	0.49	1.3	-7.9	0.691		3	-11.1	9	-9.8	Analyzed at Cal Tech
KL-Shell-1 ( rpt)	Kunlun Pass	3.6-4.2	0.49	1.3	-7.9	0.703		-1	-12.0	5	-10.6	Analyzed at Cal Tech
KLPS-15-shells	Kunlun Pass	3.6-4.2	NA	-0.9	-5.6	0.714		-4	-10.5	2	-8.9	Analyzed at Cal Tech
TB07S-25a	Zanda	5.3	0	1.0	-1.5	0.676		8	-3.6	13	-2.4	Analyzed at Cal Tech
TB07S-19a	Zanda	4.4	0.40	-0.5	-4.0	0.685		5	-6.8	11	-5.5	Analyzed at Cal Tech/Wang et al. (2013)
TB07S-6	Zanda	4	0.56	-0.6	-3.3	0.716		-5	-8.3	2	-6.7	Analyzed at Cal Tech/Wang et al. (2013)
TB07S-6a	Zanda	4	0.75	-2.4	-3.9	0.700		0	-7.8	6	-6.3	Analyzed at Cal Tech/Wang et al. (2013)
TB07S-9	Zanda	3.7	0.89	-0.1	-2.8	0.708		-2	-7.3	4	-5.8	Analyzed at Cal Tech/Wang et al. (2013)
TB07S-19b	Zanda	4.4	0	1.1	-2.5		0.707	21	-1.8	25	-1.0	Analyzed at JHU
TB07S-20b	Zanda	4.2	0	-0.3	-4.7		0.711	19	-4.4	23	-3.5	Analyzed at JHU
TB07S-20c	Zanda	4.2	0	-0.3	-2.7		0.737	10	-4.3	16	-3.1	Analyzed at JHU
TB07S-24a	Zanda	5.1	0	1.6	-1.0		0.719	16	-1.2	21	-0.3	Analyzed at JHU
TB07S-24b	Zanda	5.1	0	1.1	-1.1		0.738	10	-2.8	15	-1.6	Analyzed at JHU
TB07S-6b	Zanda	4	0	-1.2	-2.9		0.718	17	-3.1	21	-2.2	Analyzed at JHU
TB07S-9b	Zanda	3.7	0	-0.7	-2.2		0.736	10	-3.8	16	-2.6	Analyzed at JHU
TB07S-19b	Zanda	4.4	0	1.1	-2.6		0.730	12	-3.7	18	-2.6	Analyzed at UM
TB07S-19b	Zanda	4.4	0	1.1	-2.6		0.735	11	-4.1	16	-2.9	Analyzed at UM
TB07S-20b	Zanda	4.2	0	-0.3	-4.8		0.742	8	-6.8	14	-5.5	Analyzed at UM
TB07S-20b	Zanda	4.2	0	-0.3	-4.8		0.692	27	-2.9	30	-2.3	Analyzed at UM
TB07S-21b	Zanda	4.3	1.2	-2.7	-2.1		0.725	14	-2.8	19	-1.8	Analyzed at UM
TB07S-21b	Zanda	4.3	1.2	-2.8	-2.0		0.725	14	-2.7	19	-1.7	Analyzed at UM
TB07S-25b	Zanda	5.3	0.66	0.9	-2.0		0.722	15	-2.5	20	-1.5	Analyzed at UM
TB07S-25b	Zanda	5.3	0.66	0.9	-1.9		0.748	6	-4.4	12	-3.0	Analyzed at UM
TB07S-6a	Zanda	4	0.75	-2.3	-4.0		0.773	-2	-8.4	5	-6.7	Analyzed at UM
TB07S-6a	Zanda	4	0.75	-2.5	-4.1		0.744	7	-6.3	13	-5.0	Analyzed at UM

ZD0710 (TB07s-9)	Zanda	3.7	0.89	-0.2	-3.0		0.749	6	-5.5	12	-4.1	Analyzed at UM
ZD0710 (TB07s-9)	Zanda	3.7	0.89	-0.1	-2.9		0.736	10	-4.5	16	-3.3	Analyzed at UM
2 SZ 51.5	Zanda	4.2	NA	-0.4	-2.3	0.673	0.73	9	-4.1	14	-3.0	Huntington et al. (2015)
1 SZ 32	Zanda	4.7	NA	1.5	-2.4	0.685	0.74	5	-5.1	11	-3.9	Huntington et al. (2015)
1 SZ 18	Zanda	4.9	NA	0.6	-2.8	0.692	0.75	3	-6.1	9	-4.7	Huntington et al. (2015)
0.4 SZ 14.9	Zanda	5.1	NA	-7.3	18.7	0.693	0.75	2	-22.0	8	-20.6	Huntington et al. (2015)
0.4 SZ 4.8	Zanda	5.2	NA	-1.8	-1.4	0.682	0.74	6	-3.9	12	-2.6	Huntington et al. (2015)
0.3 SZ 38.25A	Zanda	5.5	NA	-1.9	-6.8	0.685	0.74	5	-9.5	11	-8.2	Huntington et al. (2015)
0.3 SZ 22	Zanda	6.1	NA	-2.6	-8.0	0.669	0.72	10	-9.5	16	-8.4	Huntington et al. (2015)
0.1 SZ 4.5	Zanda	8.5	NA	-1.1	-2.2	0.684	0.74	5	-4.9	11	-3.6	Huntington et al. (2015)

Note: Given the XRD detection limit of 0.3-0.4%, samples with less than 0.4% calcite are considered pure aragonite.

\*Data reported relative to the previous 'Ghosh' scale (Ghosh et al., 2006). Uncertainty is  $\pm 0.025\%$  (95% confidence interval).

\*\*Data reported relative to the absolute reference frame (ARF) (Dennis et al., 2011). Uncertainty is  $\pm 0.017\%$  (95% confidence interval).

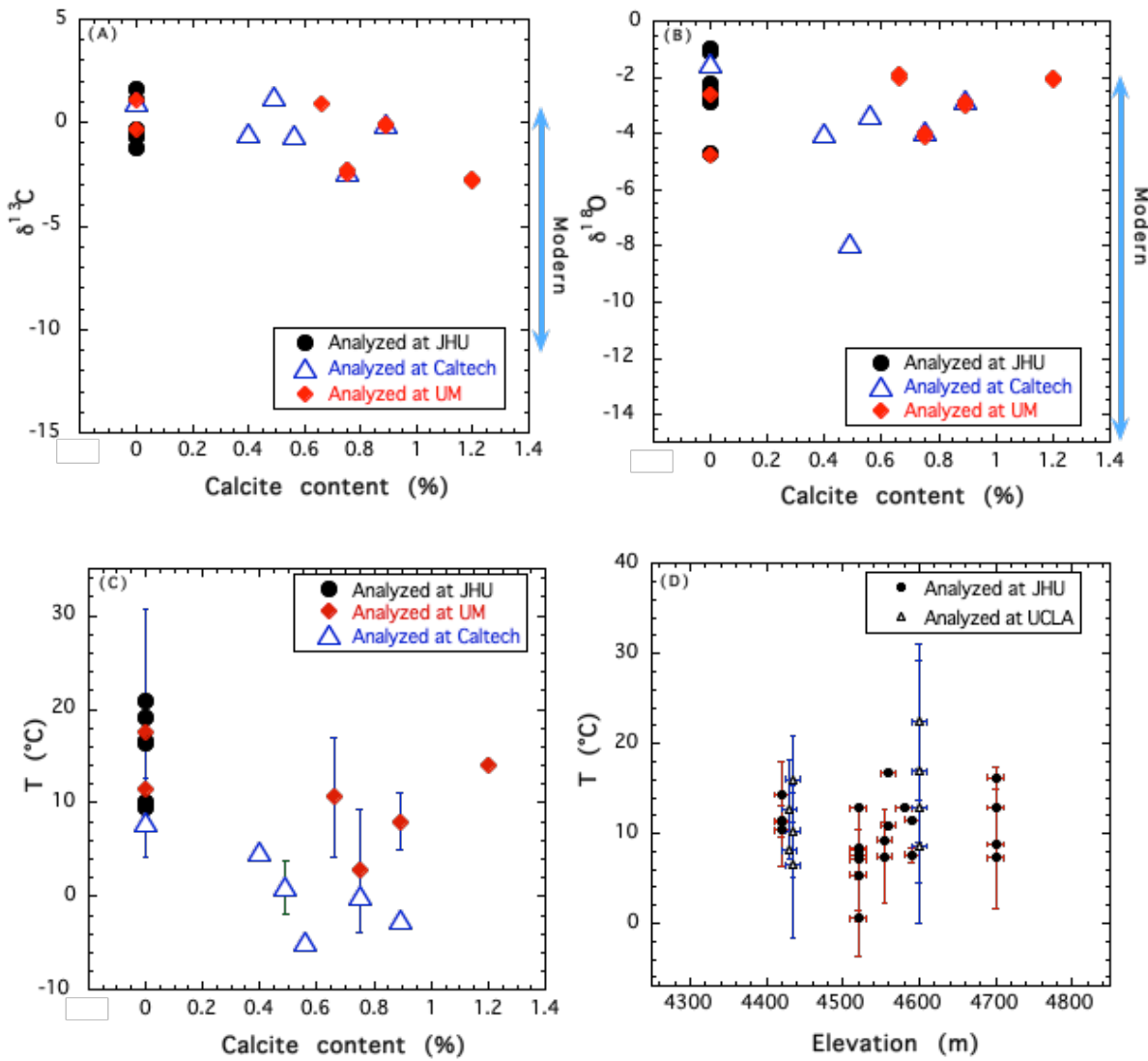
<sup>#</sup> One standard deviation from the mean of replicate analyses of the same sample.

<sup>a</sup> Temperatures calculated from  $\Delta_{47}$  values using the mollusk-specific calibration of Henkes et al. (2013):  $\Delta_{47} = 32700/T^2 + 0.3286$  for new data (on ARF scale), and  $\Delta_{47} = 31800/T^2 + 0.2737$  for  $\Delta_{47}$  data on "Ghosh" scale. Uncertainty in reported temperatures is  $\pm 6^\circ\text{C}$  (95% confidence interval).

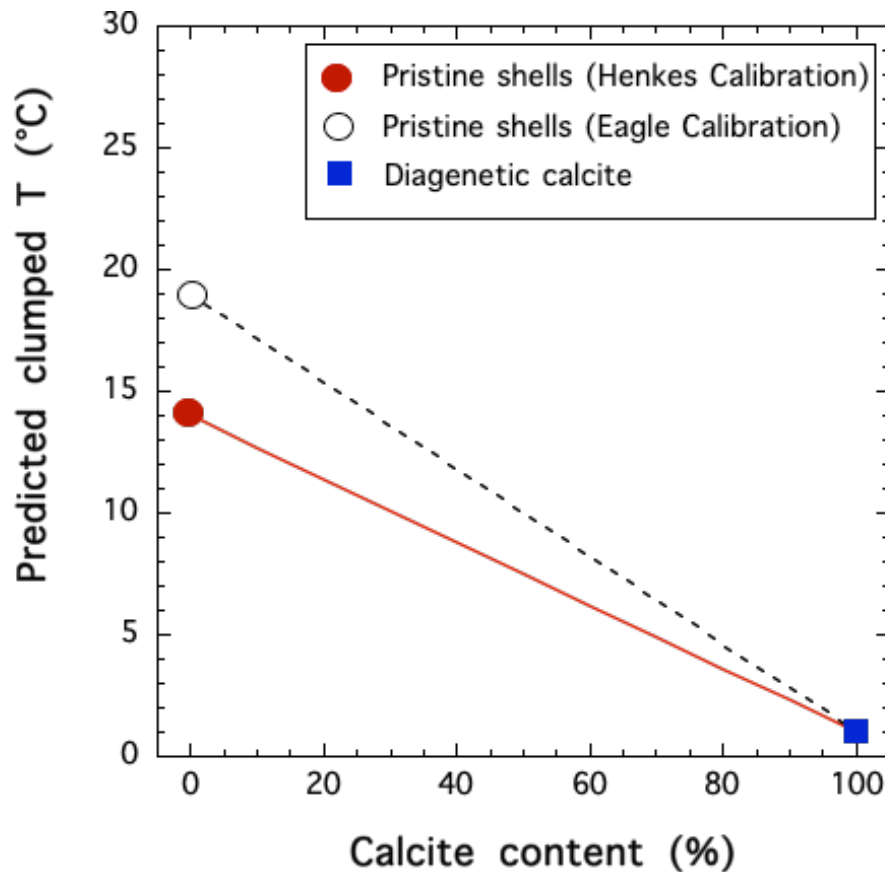
<sup>b</sup> Temperatures calculated from  $\Delta_{47}$  using the 'Aragonitic bivalve mollusks' calibration of Eagle et al (2013):  $\Delta_{47} = 40700/T^2 + 0.2483$  for new data in ARF;  $\Delta_{47} = 38300/T^2 + 0.2094$  for data on the "Ghosh" scale.

**Supplementary Table 4. Comparison of temperatures calculated using different equation**

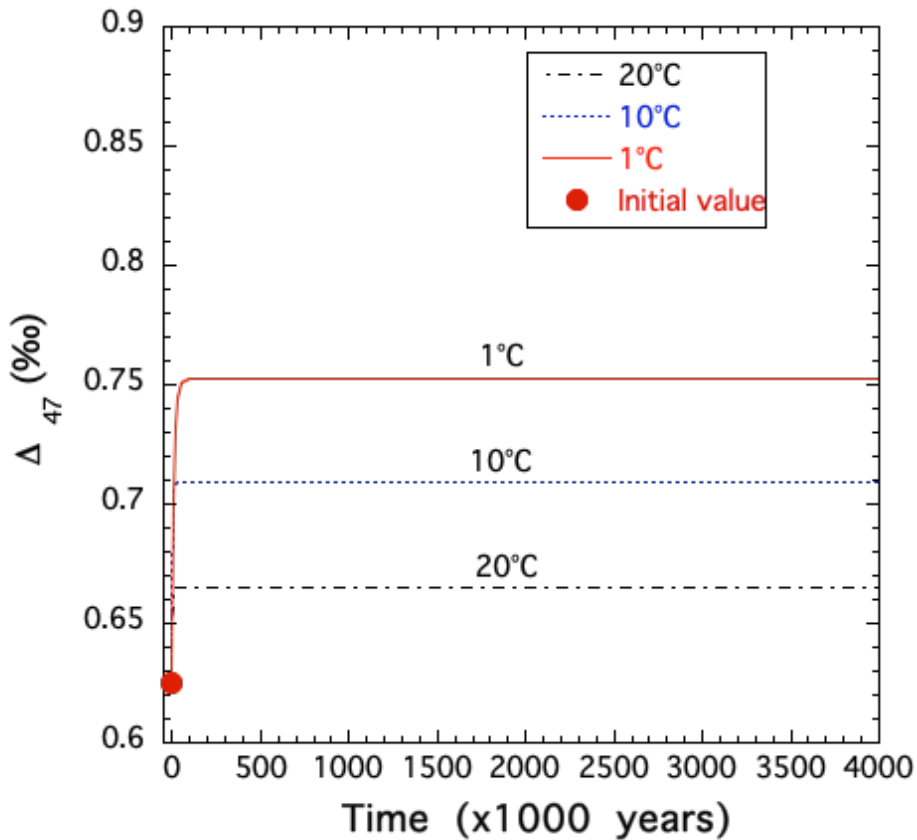
Sample	$\delta^{13}\text{C}$ (PDB)	$\delta^{18}\text{O}$ (PDB)	$\Delta_{47}$ (CDES, 25C acid digestion equivalent)	$\Delta_{48}$ (vs. HG)	T( $\Delta_{47}$ ), Heneks et al	T( $\Delta_{47}$ ), Bonifacie et al. 2017 eq. 3	T(D47), Kelson et al. 2017 , eq. 1	Petersen et al. (2019), Eq. 1
Data_783 IPL-CI-0578 TB07S-25b	0.9	-2.0	0.722	0.3330	15	13	15	14
Data_785 IPL-CI-0583 TB07S-21b	-2.7	-2.1	0.725	0.2850	14	13	14	13
Data_786 IPL-CI-0584 TB07S-20b	-0.3	-4.8	0.742	0.2110	8	8	10	8
Data_787 IPL-CI-0585 TB07S-19b	1.1	-2.6	0.730	0.4200	12	11	13	12
Data_788 IPL-CI-0586 TB07S-6a	-2.3	-4.0	0.773	0.3720	-2	0	2	0
Data_789 IPL-CI-0587 ZD0710	-0.2	-3.0	0.749	0.2710	6	6	8	6
Data_838 IPL-CI-0633 TB07S-21b	-2.8	-2.0	0.725	0.2250	14	13	14	13
Data_840 IPL-CI-0634 TB07S-25b	0.9	-1.9	0.748	0.3360	6	6	8	6
Data_841 IPL-CI-0635 TB07S-20b	-0.3	-4.8	0.692	0.2330	27	22	24	24
Data_842 IPL-CI-0636 TB07S-19b	1.1	-2.6	0.735	0.1530	11	10	12	10
Data_851 IPL-CI-0650 ZD0710	-0.1	-2.9	0.736	0.2820	10	10	11	10
Data_855 IPL-CI-0655 TB07S-6a	-2.5	-4.1	0.744	0.2000	7	7	9	8



Suppl Fig. 1. Comparison of analysis results for fossils (A-C) and modern shells (D) analyzed in different labs. The double arrows in (A) and (B) indicate the variation ranges of  $\delta^{13}\text{C}$  and  $\delta^{18}\text{O}$  values, respectively, of modern shells. Temperatures shown in (C) and (D) were calculated using the Henkes et al. (2013) calibration. The error bar indicates 1 standard deviation from the mean of replicated analyses of a sample. Some of the fossil samples analyzed at Caltech and John Hopkins University (JHU) were re-analyzed at University of Michigan (UM), yielding the same  $\delta^{13}\text{C}$  and  $\delta^{18}\text{O}$  values and similar  $\Delta_{47}$ -derived temperature values for the same samples (A-C). Analysis of additional modern samples from two of the study lakes at UCLA also produced similar results to those from the JHU lab for the same lakes except two samples (D). The results from these two samples analyzed at UCLA were not used because their replicates yielded not only very large temperature ranges (much larger than the reported analytical uncertainty) but also unreasonably high temperatures (see text for explanation).



Suppl. Fig. 2. Effect of mixing diagenetic calcite with pristine aragonite on the  $\Delta_{47}$ -derived temperature of aragonite shell predicted using a simple two component mixing model. The model assumes that calcite was formed at near freezing temperatures ( $1^{\circ}\text{C}$ ) characterizing the present-day high elevation environment in the study area and the temperature of unaltered aragonite was the average temperature determined from the  $\Delta_{47}$  values of our pristine fossil shells from Zanda Basin in southwest Tibet.



Suppl. Fig. 3. Modeled  $\Delta_{47}$  evolution at low diagenetic temperatures using Eq. (3) in Staudigel and Swart (2016) and rate constants calculated by the Arrhenius Equation. The following Arrhenius parameters estimated by Staudigel and Swart (2016) were used to calculate the rate constants at different temperatures:  $E_a = 1.1 \times 10^5$  J/mol and  $\ln(k_0) = 21.7$ . The initial  $\Delta_{47}$  value used in the model was 0.625 and the equilibrium or “annealing” values were calculated using the revised carbonate equation given in Zaarur et al. (2013):  

$$\Delta_{47} = (0.0526 \pm 0.0025) \times 1000000/T^2 + (0.0520 \pm 0.0284)$$
.